INVESTIGATION OF ACCURACY IN QUANTITATION OF ^{18}F-FDG CONCENTRATION OF PET/CT

A Thesis

Submitted to the Graduate Faculty of the
Louisiana State University and

Acknowledgements

I would like to acknowledge the support and guidance

Thanks to Rajesh Manoharan, another graduate student who worked at the PET center with me. He was not only helpful to me in acquiring PET data but also helped me in many ways, especially during the last semester of my rotation at the MBPCC.

Many people have encouraged and helped me to continue my graduate study at Louisiana State University and the MBPCC. Only a few names have been mentioned here.

I thank Michael Domingue, my husband, for his great patience and support during my graduate study.

Finally, I am grateful for the financial support of Louisiana State University Board of Regents, providing my graduate fellowship.

Table of Contents

Acknowledgements.....ii

Abstract.....v

Chapter 1. Introduction……..…….....1
1.1 Motivation……..1
1.2

Abstract

The PET/CT scanner has been recognized as a powerful diagnostic imaging modality in oncology and radiation treatment planning. Traditionally, PET has been used for quantitative analysis, and diagnostic interpretations of PET images greatly relied on a nuclear medicine physician's experience and knowledge. The PET data set represents a positron emitter's activity concentration as a gray scale in each pixel. The assurance of the quantitative accuracy of the PET data is critical for diagnosis and staging of disease and evaluation of treatment. The standard uptake value (SUV) is a widely employed parameter in clinical settings to distinguish malignant lesions from others. SUV is a rough normalization of radioactive tracer uptake where normal tissue uptake is unity. The PET scanner is a sensitive diagnostic method to detect small lesions such as lymph node metastasis less than 1 cm in diameter, whereas the CT scanner may be limited in detecting these lesions. The accuracy of quantitation of small lesions is critical for predicting prognosis or planning a treatment of the patient. PET/CT uses attenuation correction factors obtained from CT scanner data sets. Non-biological materials such as metals and contrast agents are recognized as a factor that leads to a wrong scaling factor in the PET image. We challenge the accuracy of the quantitative method that physicians routinely use as a parameter to distinguish malignant lesions from others under clinical settings in commercially available C

Chapter 1

Introduction

1.1 Motivation

The hybrid system of a PET scanner combined with CT scanner (PET/CT) has gained popularity in the oncological community since its commercial introduction to the market in early 2001 [1]. The integrated PET/CT unit superimposes PET images on CT images with minimum co-registration problems between the two images by minimizing patient movement. Simultaneously providing anatomical information by CT scan helps physicians to identifyl inform

hypoxic cell groups, which are more resistant to radiation therapy and more likely to be a source of distant metastasis or recurrence in the future. This suggests a unique role for PET in oncology treatment planning by distinguishing more resistant cell groups from the others; using PET for targeti

Our question is: “How reliable are these SUV values?” PET scan images use gray scale maps to depict activity concentrations of a positron emitting source in the body. We decided to investigate major factors that can adversely alter SUV. The normalization process to an individual patient in Equation 1, where one divides by uniform distribution of the normal tissue, causes more error. Each individual has different metabolism of the tracer. Distributions of the activity concentration reflect an individual’s physiological function. Therefore, we ignored the denominator of Equation 1 and only concentrated on activity concentrations (the numerator) that are utilized to calculate SUV.

Many factors affect quantitative accuracy of the PET/CT; some are particularly unique to hybrid PET/CT scanners [1, 13, 14]. The scaling problem of attenuation values (μ) at 70 keV into 511 keV is an inherent problem for the PET/CT unit. The μ is an energy-dependent value. The attenuation correction factors are obtained from a CT scan at a mean energy of 70 keV and scaled into a μ at 511 keV by a manufacturer-dependent algorithm [1].

One problem is oral and intravenous iodinated contrast materials are commonly used in CT. They enhance attenuation in the gastrointestinal tract and in vessels to assist visual discrimination of these anatomic structures. This contrast can create artifacts in both the CT image and CT-based attenuation correction of the PET image [15-17].

Partial volume effect is another factor that affects quantitative analysis in PET. The volume of the object, relative to the spatial resolution of the imaging system, affects the recovery of activity concentration of PET and single photon emission computed tomography (SPECT). This effect has been discussed extensively for PET and SPECT brain research studies [18]. It is critical in a malignancy, such as glioblastoma

maltiforme, where a physician is interested in whether recurrent tumor is present compared to the normal cortex. We noticed that this partial volume effect of the PET/CT scanner is not widely considered when it comes to image interpretation in oncology settings.

Another issue that we did not cover in this thesis is organ movement. Physiological activity such as respiration, heart beat, and bowel movement are problematic [13, 19, 20]. Sometimes anatomical location of the lesion is disregarded because of artifacts created by physiological motion. Diagnosis of the patient with lesions at the base of the lung and the dome of the liver is particularly difficult. To solve respiratory motion, respiratory-gated PET scanning is under research development [21, 22].

Physicians are advised to review two sets of fused PET/CT images, using both attenuation corrected PET and non-attenuation corrected PET images [13]. One of the issues that PET/CT is facing is

artifacts mentioned above and also the partial volume effects. Further, we search to understand the limitations of PET/CT in the clinical settings.

1.2 Organization of the Thesis

Chapter 2 describes basics of PET/CT physics and instrumentation to understand the performance of the scanners. Chapter 3 describes the performance of the PET/CT scanner we tested including counting-rate characteristics and uniformity of response. Chapter 4 discusses the effect of contrast agents on attenuation-correction accuracy. Chapter 5 describes an investigation of partial volume effects and possible methods to recover activity concentrations. The final chapter provides a summary of the work and a brief discussion of potential future research directions.

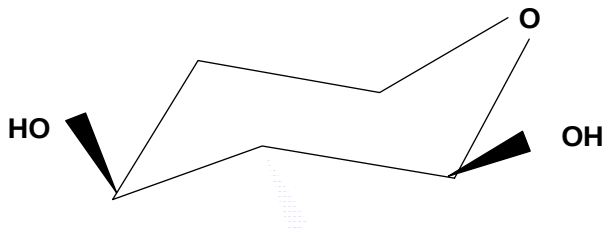
O
HO
OH

electrons, elastic scattering with atomic electrons, inelastic scattering with a nucleus, or elastic scattering with a nucleus. The positron takes a torturous passage through matter, which complicates the estimation of range. Eventually, the positron and an electron may form a metastable intermediate species, positronium. The electron and positron revolve around their center of mass; positronium's half-life is about 10^{-7} seconds. The positronium formation occurs in about one-third of cases in water or human tissue while direct annihilation occurs the rest of the time [23].

When the positron and electron annihilate, they give off electromagnetic radiation. The most probable mode is rest mass converted into two photons of 511 keV each, propagating at 180 degrees to conserve momentum when the positronium has no residual kinetic energy (Figure 2-1). This principle is used to determine the line of response in the PET scanner. At less than 1% probability, three photons can be emitted. Also, not all annihilation events are zero-momentum; to safisfy momentum-conservation, these photon pairs are not exactly emitted at 180 degrees (a maximum deviation of ±0.25 degrees) [24]. In water, about 65% of annihilations deviate from co-linearity. This effect contributes resolution blurring of 1.5 mm to 2.0 mm for 80 cm to 90 cm diameter PET rings [23, 24].

There are several nuclides used in PET: ^{11}C ($T_{1/2}$: 20.3 min, max range in water: 5.4 mm) ^{13}N (9.97 min, 5.4 mm)), ^{15}O (124 sec, 8.2 mm), and ^{18}F (110 min, 2.4 mm). ^{18}F-FDG is the predominantly used radionuclide for PET imaging because of its relatively long half life.

Nuc

- **Compton Scattering**

undesirable effects on X-ray imaging because it introduces image contrast variations depending on the photon paths in addition to the object attenuation properties.

An X-ray CT detector operates in charge-integration mode and does not have energy discrimination, unlike a nuclear medicine detector. PET detectors operate in single-photon counting mode and have energy discrimination, ideally allowing rejection of scattered photon counts.

2.1.4 True, Random and Scattered Events

- **True and Random Events**

To be considered a valid event, the PET scanner must detect two 511 keV events simultaneously in two different detectors (Figure 2-3). The system assigns a line of response (LOR) for coincidence events, a straight line connecting the two detectors. Ideally, the positron annihilated somewhere along this LOR.

The difference in time window (Figure 2-4) is set under consideration of the following factors: time of travel of two annihilation photons, the detector's scintillation time, and the electronics' processing time. The scintillation time affects the time resolution, which is the uncertainty in the timing characteristics due to fluctuation of scintillation decay. A detector with short scintillation time constant has a small timing resolution. The maximum difference for time of travel by each photon before interaction in the detectors is about 3.33 ns using speed of light ($3x10^8$ m/s) and for a 1 meter scanner diameter. At time T, if detector 1 produces a signal, then any signal produced by detector 2 between $T+\tau_c$ and $T-\tau_c$ is considered a coincident event. The resolving time of the circuit is the coincidence time window and expressed as $2\ \tau_c$.

Random events occr Tm(e)Tj12 0 nt even

From this equation, the total random rate is approximately proportional to the square of total count rate for all detector pairs. To minimize random

590-665 keV. BGO crystals have worse energy resolution compared to NaI(Tl) crystals. A typical BGO scanner's energy window is set from 300-350 keV to 650 keV. [24].

One of the methods to reduce scattering events is use of lead or tungsten septa (i.e. 2D mode). In multi-ring scanners, septa reduce scattered photons reaching the detectors. Septa also reduce the sensitivity of the scanner. Another method is to mathematically correct scattering events by using object-scatter models; however, scatter is very object-dependent. Currently, simple but computationally efficient models are used, but these are inherently limited in their accuracy. Monte Carlo methods can provide more realistic models but are too computationally intensive for clinical practice; recent developments of acceleration techniques eventually may make Monte Carlo methods feasible for clinical practice [27].

2.1.5 Sensitivity and Depth of Interaction

The sensitivity of a PET scanner is determined by its geometry and detector stopping power. The ideal geometry of PET scanners is (1) a small diameter and large axial field of view (FOV), and (2) a scintillation detector with high stopping power and high energy resolution. After a photon enters the detector, it travels a short distance before depositing its energy. Typically, the event registers the LOR as a connection of two points on the entrance surfaces of the detectors rather than the two actual interaction points. The error from this assumption becomes large when the photons enter at an oblique angle and with thick detectors. This parallax error is worst when annihilation occurs in the periphery of the scanner's FOV. The thickness of the detector trades off sensitivity and stopping power with parallax error. Detectors providing depth-of-interaction measurement are under research, e.g. [28].

2.2 Photon Attenuation and Attenuation Correction Factors

2.2.1 Attenuation Correction Factors

Suppose the scanned body consists of a homogeneous material, and d_1 and d_2 are the distance each annihilation photon traveled th

transmission data from coincidence events]; (2) γ-ray Sources: ^{137}Cs [a γ

up to 30%); replacing by a single attenuation coefficient at 511 keV potentially introduces an error [25].

- ## Scaling

The images created by CT are approximately linearly correlated to the attenuation coefficients of soft tissue. CT values multiplied by the ratio of the attenuation coefficients at 511 keV and at mean CT energy are called scaling [1, 25]. For low-Z material, the approximation of the attenuation coefficient is accurate when multiplied by scaling factors. However, different scaling factors are necessary for bones, because linear scaling is a poor approximation. This

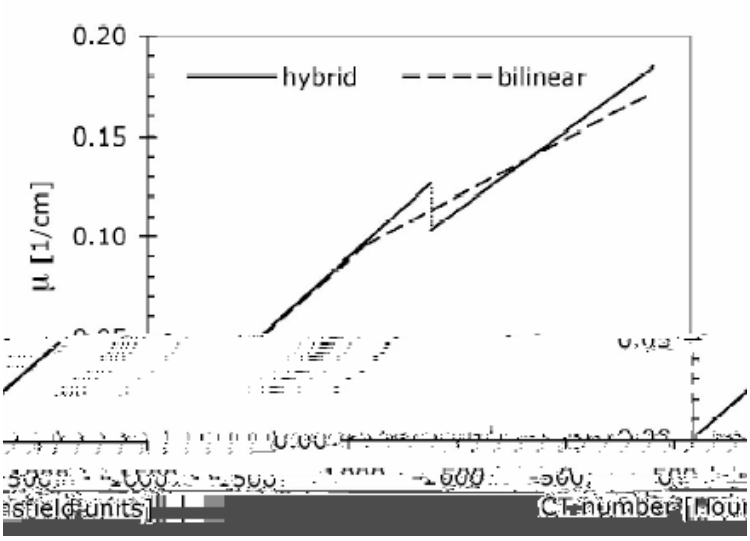

Figure 2-7: Conversion of CT numbers to linear attenuation coefficients at 511 keV. The hybrid me

arms may be raised during the CT scan. For a large patient, some part of the body may be outside the CT's FOV, resulting in some bias of the reconstructed activity distribution due to erroneous ACFs [13].

- **Metal Implant**

Many oncological patients have metal implants such as chemotherapy ports, pacemakers, dental fillings, and artificial joints. These high-Z materials cause significant artifacts in the attenuation correction factor obtained in the CT energy range. It is especially important to reconstruct attenuation uncorrected images in these patients.

- **Contrast Agents**

Intravenous (IV) contrast agents are composed of iodine (Z=53) at concentrations of 300-380 mg/mL. Typically, 100-200 mL of IV contrast agent is injected as a bolus at a rate of 1.5 to 5 mL/s [25]. The distribution of contrast agent depends on the time after injection. Over time, the agent is excreted through the kidneys, ureters, and bladder. Oral contrast agents are either barium (Z = 56) based or iodine based. Because of increased attenuation due to high Z, these contrast agents produce contrast in a CT image.

Immediately after a bolus injection, the CT numbers of highly vascularized tissue increase to 200-300 from 30-60. At 511 keV the mass attenuation coefficient of iodine is about the same as water or soft tissue (Figure 2.8). Therefore, any scale factor that correctly predicts the attenuation factor at 511 keV for bone or soft tissue will overestimate the attenuation at 511 keV for contrast agents [25]. According to recent literature, intravenous contrast at normal concentrations has little effect on the CT-based ACFs, but for oral contrast, larger intestinal volumes and a wide range of concentration (about 170 HU in the stomach, about 700 HU in lower gastrointestinal tract where water

is absorbed) can potentially cause overestimation of ACFs [1]. A recently-proposed approach to avoid over-estimation of ACFs is, for pelvic gastrointestinal oral contrast agent, the use of negative oral contrast agent [13].

PET/CT scanners. 3D iterative reconstruction is independent of geometry, but it is computationally intensive. Hybrid algorithms combine efficient 2D iterative algorithms with a fast rebinning algorithm, where 3D data is reduced into 2D data.

2.3.2 2D Data

- **Analytic 2D Reconstruction**

The Radon transform of an object $f(x,y)$, denoted as $g(s,\phi)$, is defined as its line integral along a line inclined at an angle ϕ from the y-axis and at distance *s* from the origin.

Mathematically, it is written as

$$g(s,\phi) \equiv \Re f(x,y) = \int_{-\infty}^{\infty}\int_{-\infty}^{\infty} f(x,y)\delta(x\cos\phi + y\sin\phi - s)dxdy \quad (10)$$

where $\Re$ is the Radon transform operator.

In medical imaging, we are interested in recovering $f(x,y)$ from the sinogram $g(s,\phi)$, which is the measured PET data, after corrections for scatter, randoms, and attenuation.

Associated with the Radon transform the back-projection operator is defined as

During reconstruction, filtering or deconvolution is used to remove the PSF blurring, recovering the original object *f(x, y)*. Details of the FBP reconstruction methods can be found in imaging textbooks [30, 31].

- ## Iterative Reconstruction

Filtered backprojection is computationally efficient. It is based on the assumption that the projection images are perfect projections of a three dimensional object. This is not true: Compton scattering, and photon attenuation factors in the patient affect the LORs. Iterative reconstruction has been developed to overcome this problem. An initial activity distribution in the patient is assumed, and then projection images are calculated from the assumed activity distribution. The calculated projection images are compared with the actual images and the assumed activity distribution is modified and recalculated [32].

The most widely used iterative algorithms in PET are the maximum-likelihood expectation maximization (ML-EM) algorithm and its accelerated version OSEM. OSEM was proposed in 1994 and is sufficiently fast for clinical applications. With each iteration, the target function is updated several times, proportionally accelerating i

Rebinning is a method to estimate 2D transaxial sinograms from oblique sinograms acquired in 3D mode. Two rebinning approaches are commonly used: single-slice rebinning (SSRB) and Fourier rebinning (FORE) [23]. SSRB assumes that each measured oblique LOR only traverses a single transaxial section within the support of the tracer distribution and average overall available estim

Chapter 3

Uniformity of Activity Concentration of Discontinuous Positron Emitting Sources

m

Approximately 20% of ^{18}F-FDG appears in the bladder. The remaining activity in the body is about 6 mCi at the time of scanning. Typical whole body PET uses 6 bed positions. Ignoring the lower body, the rest of the body is about 4 PET beds. Then neglecting the scattering from outside of FOV, approximately 1.5 mCi of activity is located in one PET bed. Comparing to Figure 3-1, a 10 mCi dose is likely to be under saturation of the PET scanner's true counts.

As described in the instrumentation section, BGO crystals have good stopping power, but poorer light yield and resolution than NaI(Tl) crystals. BGO crystal's energy resolution is 25%; LLD is set to 350 keV; and ULD is set to 650 keV. A 3D PET scanner does not have septa between the BGO crystals. A 3D mode acquisition improves statistics by increasing the number of counts, but at the expense of increased scattered and random events.

Accepting more counts has an advantage for patients by reducing tracer activity and reducing acquisition time. However, 3D mode image reconstruction is computationally intensive. Furthermore, the 3D mode suffers from blurring of images by accepting more scattering events as true counts. This problem is not only from inside of FOV but also from outside of the FOV. This may cause problems in image quality: organs located outside of FOV with high ^{18}F-FDG concentration such as brain or bladder possibly contribute scattered events into the FOV.

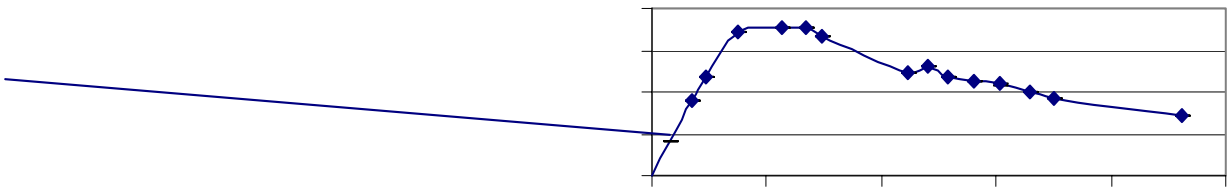

The normalization method assumes that the normalization coefficients are applicable to discrete sources, such as one finds for lesions in the clinical setting. This is a critical assumption for accurate quantitative analysis. We scanned a 1 mL uniform source over the FOV as a pilot study. The source was composed of

3.2.2 Materials and Method

Twenty-one micro-centrifuge tubes (inner diameter 9 mm; height 35 mm) were arranged in a Styrofoam disk (diameter 20 cm, thickness 2.5 cm) as shown in FigF a Styrer 20 cm

and 512 x 512) were derived from the same data set. The maximum activity

A

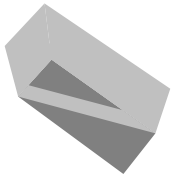

Sources placed in X-Y plane showed higher variation in activity concentration compared to ones in X-Z and Y-Z plane. The

process. However, the normalization processes are done daily by manufacturer-created routine QA software and we did not have access to data to understand what exactly this software is doing for normalization. To conclude whether another discrete source normalization process will improve accuracy of quantitation of the PET/CT scanner or not, extensive collaboration with the manufacturer is probably necessary.

Chapter 4

Contrast Agents and PET/CT Data

4.1 CT Numbers or Hounsfield Units (HU)

CT numbers are quantitative. CT numbers are used to identify the composition of a structure or lesion such as lung or bone. After CT reconstruction, CT number represents the relative attenuation coefficient of the tissue in that pixel, according to the formula [32]

$$CT(x,y) = 1000 \times \frac{(\mu(x,y) - \mu_{water})}{\mu_{water}} \qquad (14)$$

CT numbers are called “Hounsfield units” (HU). The CT images typically possess 12 bits of values ranging from -1000 to +3095

(air: -1000, soft tissue: between -300 and -100, water: 0, dense bone: +3,000).

4.2 Contrast Agents and Attenuation Correction Factors

4.2.1 Introduction

The benefits from the administration of contrast agents are significant especially

Theoretically, these overcorrected values could possibly lead to false representations of the PET images [35, 36].

The majority of patients undergoing PET/CT are oncological patients and it is not infrequent for a patient to have a fluoroscopic study, receiving contrast agent for screening for gastro-intestinal (GI) malignancies, prior to the PET/CT scanning. Sometimes residual contrast agents in the GI tract are recognized after a topogram (patient-positioning) scan during PET/CT studies. Fluoroscopic contrast causes significant problems because a higher density of barium sulfate is used for these GI radiographs.

In PET, the standard uptake value (SUV) is widely used to quantitatively distinguish a malignant lesion from a benign lesion. The artifacts due to wrong HU scaling by contrast agents possibly may mislead physicians' interpretations of the PET/CT image. To investigate the effect of contrast material on SUV, first we tested HU for different dilutions of commonly used contrast materials. Second, we investigated its effects on recovered activity concentration.

4.2.2 Materials and Methods

Three types of commercial contrast agen

- **Experiment 2**

Gastroview™ and Omnipaque 300™ were prepared in a series of dilutions of 0, 1, 4, 10, 20, 30, 40, 50, 60, 80, and 100% (v/v) as explained in Experiment 1.

A 1.0 mL volume of diluted contrast material was pipetted into 1.5 mL polyethylene micro-centrifuge tubes (0.9 cm inner diameter), and arranged in a micro-centrifuge rack. The tubes were arranged in columns spaced at 2.4 cm, 4.0 cm, and 5.6 cm from center of the rack and FOV as illustrated in Figure 4-3.

A stock solution of ^{18}F-FDG was prepared at the concentration of 109.6 μCi/mL. A 10 μL volume of ^{18}F-FDG was pipetted into the 1 mL solution in each tube (1.1 μCi/mL). Different contrast concentrations were arranged in the Z-direction because we know that the variation of the measured activity concentration is less in this direction from the experiment in section 3.1.2.

PET images were acquired on the Reveal HD scanner using the default Thoracic protocol, except the slice thickness was set to 2 mm. The image data were viewed with the PET/CT scanner software and the maximum pixel value of each object was recorded.

For comparison, images were also acquired using a GE Discovery ST PET/CT scanner (The GE Discovery ST is owned by Mary Bird Perkins Cancer Center) in the same experimental setting except the slice thickness was set to 3.75mm.

dilution produced maximum error is unknown. We did not measure the variation of activity concentration across the FOV for this scanner. The GE scanner uses septa to acquire 2D mode data, unlike the Reveal scanner. With the different concentrations arranged in the axial direction of the gantry, it is possible that subtle differences in the position of objects in relation to the septa affect the potential sensitivity. Further investigation of the GE scanner was viewed as an extension to the primary purpose of this thesis. In the future one should investigate the effect of 2D vs. 3D acquisition modes on system response uniformity. The GE scanner is capable of retracting its septa to acquire data in 3D mode, so it would be an ideal platform for further investigation.

A recent clinical study reported that the PET artifact by an intravenous contrast material was limited to the thoracic veins containing undiluted contrast agent [36]. They also found that patients with artificially high uptake values have statistically smaller body surface area than patients with no artifacts. Another possible cause of artifacts is that bolus IV contrast passages are imaged in the CT scan but when the PET data are acquired subsequently, the high concentration of the contrast materials has redistributed throughout the body.

Another group reported that high density barium oral contrast used for some GI studies can potentially overcorrect ACFs, but ired

171±45 HU in stomach to 263±24 HU in ileum. They demonstrated overestimation of activity concentrations (for gastrographin 20%; barium 21%). For 50% dilution of barium, a typical concentration used in colonography, the over-estimation of activity concentration was 580% [38].

These studies indicated that if the administered volume of intravenous contrast ma

A

- **Partial Volume Effect**

In ideal quantitative PET, the image should represent the distribution of radioactive tracer concentration as a size-invariant function. Partial volume effect causes a small object, less than twice the spatial resolution of the imaging system, to have reduced signal amplitude [18, 23, 40]. This effect has been widely addressed in brain research where quantitative analysis of small areas of abnormal cortex within normal tissue is critical. If object size affects accuracy of tracer activity concentration recovery, we need to know the limitation of the method in an oncological setting. An inaccurate recovery of small lesions affects diagnosis and evaluation of the malignant lesions. Surprisingly, partial volume effects are not widely discussed in textbooks or review articles related to diagnosis of malignancy using PET/CT. Little information was found in the literature about the influence of partial volume effect on maximum pixel value measurements, such as one uses in clinical settings to calculate SUV. We tested several different sizes of spheres and sought to identify the critical object size that results in significant error in recovered activity concentration for diagnosis in the oncological setting.

5.1.2 Materials and Methods

A 0.4 μCi/mL (14800 Bq/mL) activity concentration of ^{18}F-FDG was prepared in a volume of 50 mL water. Four different diameters of plastic spheres (10 mm, 14 mm, 18 mm, and 23 mm inner diameters) were arranged on a 6 cm radius circle on the scanner's X-Z plane. The objects' centers were evenly spaced. For each diameter, three identical sizes of spheres, except for the largest 23 mm sphere, were arranged alternately and two

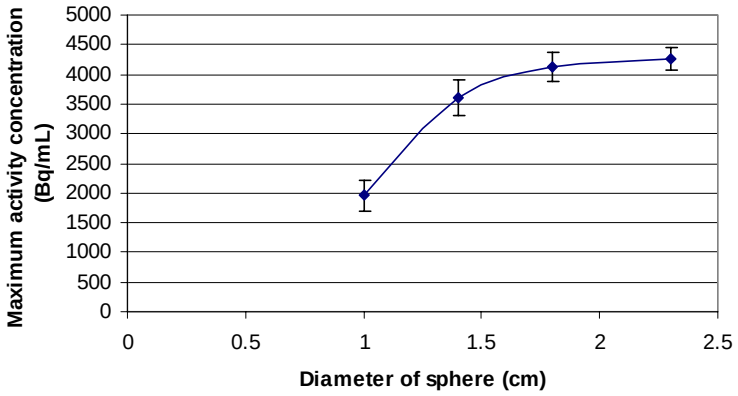

Figure 5-1: Maximum activity concentration as a function of sphere diameter. The 1.0 cm sphere recovered an activity only 46% of th

does not guarantee uniform activity distribution across patients, because there are

One can imagine as two objects get close to each other, the activity concentration distributions overlap and alter the recovered values.

We chose spheres because lesions that we are interested in such as lymph nodes

maximum activity concentration profiles. The slices with the maximum activity concentration were identified. The maximum activity concentration was analyzed as a function of position in the image profiles.

- **Experiment 2**

Three spheres were positioned at the center of FOV along the X-axis. We only tested the 10 mm sphere because we already know that the 18 mm sphere gives relatively accurate recovery of activity concentration from Experiment 2 of Chapter 5.1. Three identical 10 mm plastic spheres were aligned on the X axis at the center of FOV. The outer walls of the spheres were separated by 0 mm and images were acquired with the CTI-Siemens PET/CT scanner as described in Chapter 3. The activity concentration was 0.2 μCi/mL (7400 Bq/mL). The same raw data were reconstructed three different ways into images. The methods were (a) OSEM 4i8s, FORE, 128 x 128 matrix; (b) FBP with Gaussian filter with 3mm FWHM, 128 x 128matrix; (c) FBP with Gaussian filter with 3mm FWHM, 512 x 512 matrix. Attenuation uncorrected image files formatted in DICOM were analyzed using IDL 5.6 student edition (Research System Inc., Boulder, CO). For each transaxial slice, each column was searched for the maximum pixel number to created image profiles. All trans-axial slices were examined and the slice that gave the maximum pixel numbers was selected and multiplied by the rescaling slope found in the DICOM file to calculate maximum activity concentration. Activity concentrations were analyzed as a function of position across the scanner FOV.

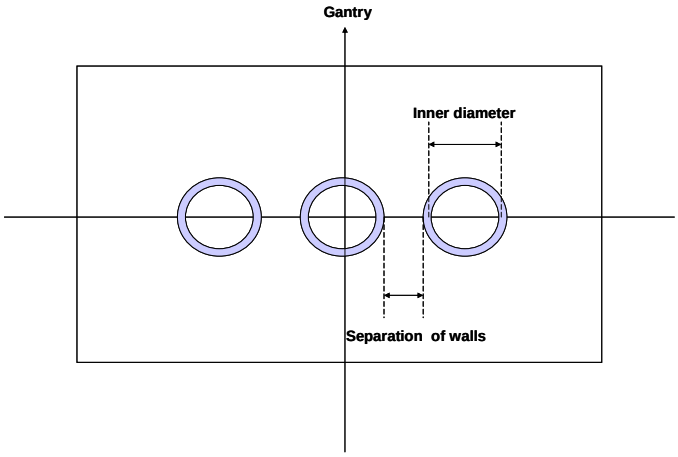

Figure 5-2: Arrangement of three identical hollow spheres. The separations of the objects were measure in separation of outer walls. The center sphere was located at the center of FOV. The three balls were arranged in tandem along the X-axis.

5.2.3 Results and Discussion

- **Experiment 1**

The results are shown in Figure 5-3. Variations in maximum activity concentrations were greater in 10 mm spheres than in 18mm spheres. This is probably due to the partial volume effect that we discussed previously. For a small object, only a small number of pixels compose its im

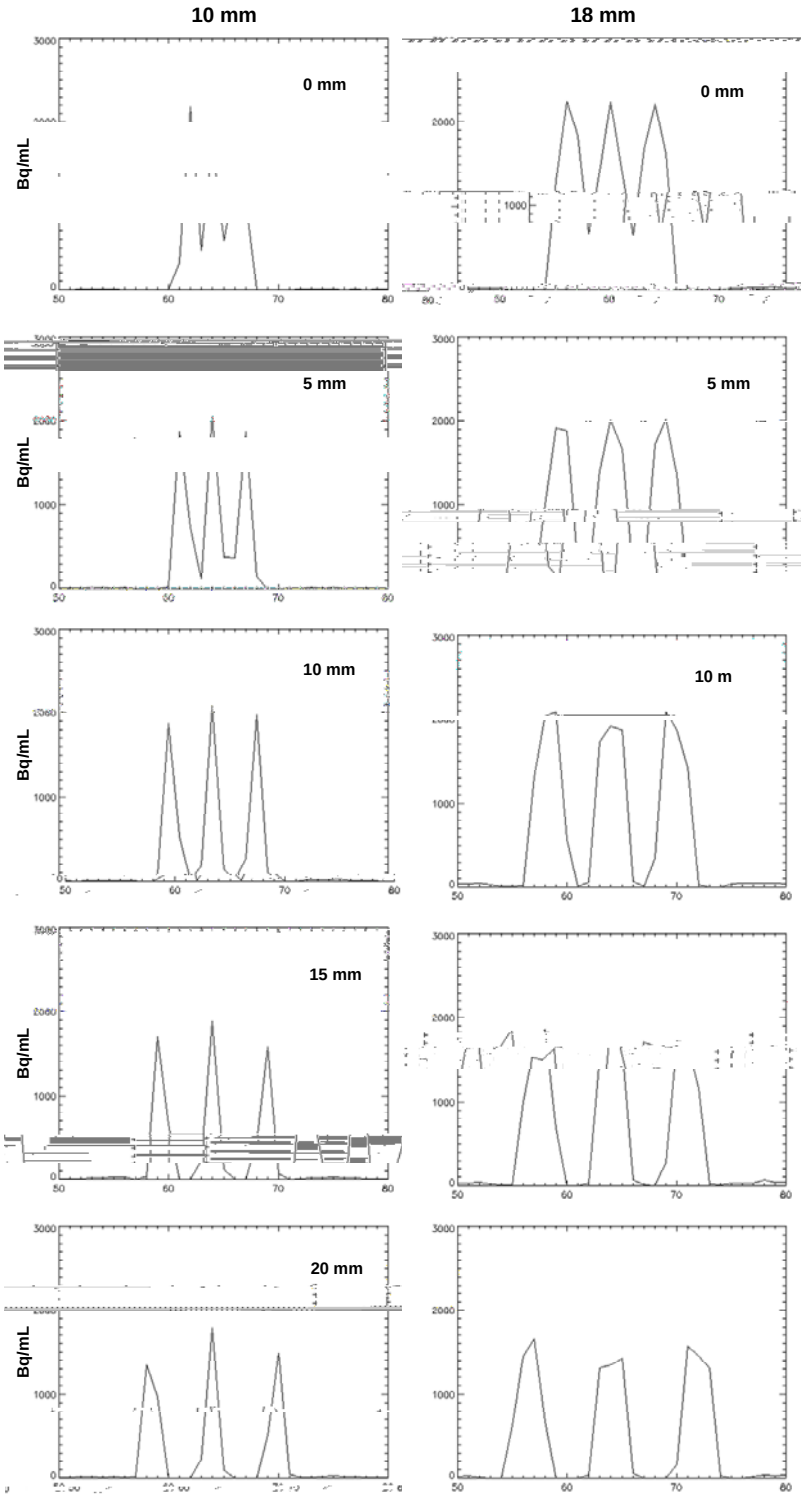
10 mm
18 mm
0 mm
0 mm
5 mm
5 mm
10 mm
10 m
15 mm
20 mm
Bq/mL

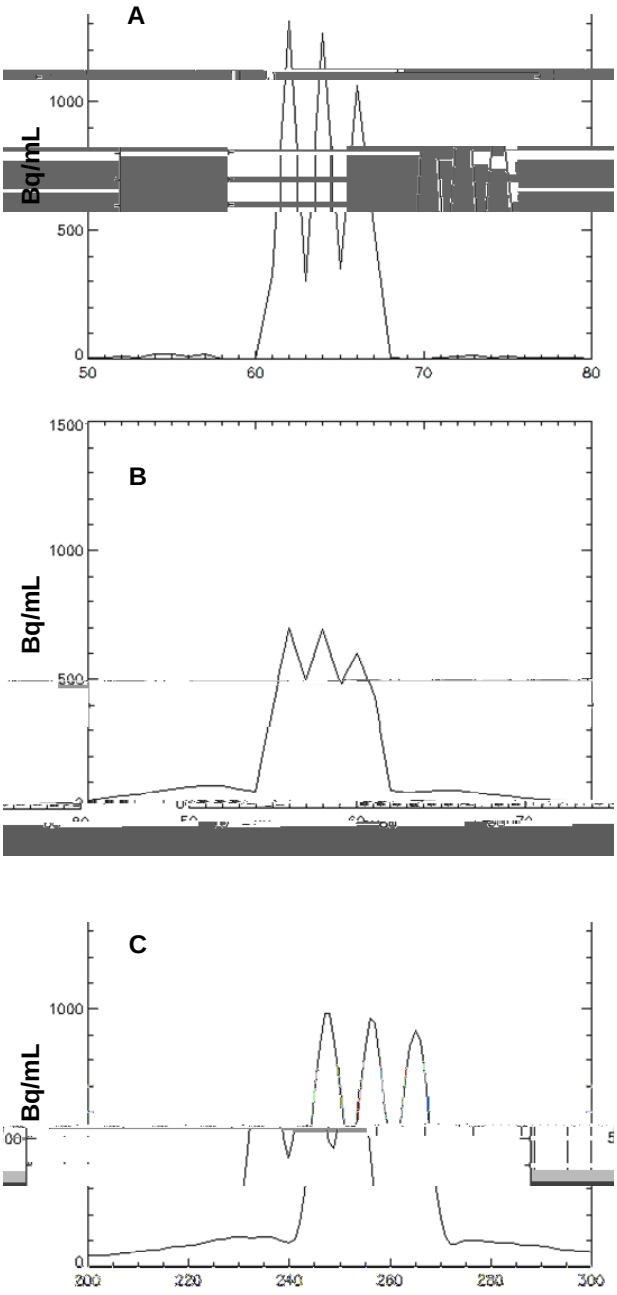

Figure 5-4: Maximum activity concentration recovery for three spheres arranged in tandem are plotted as a function of position in X-direction. Three different image reconstructions were tested on the same raw data. A: OSEM 4i8s 128 x 128matrix, B: FBP 128 x 128 matrix, and C: FBP 512 x 512 matrix. Outer walls of the spheres are spaced without any gap.

Chapter 6

Conclusions

In Chapter 3, we demonstrated that the currently available clinical PET/CT scanner does not guarantee accurate recoveries of activity concentrations with clinical scanning modes. The normalization process of the PET scanner using a continuous volume source does not lead to an accurate normalization of discrete small sources in the FOV. Also the image reconstruction parameters should be optimized by further investigations.

In Chapter 4, we tested one of the possible factors, contrast agents, that might affect quantitation of the PET/CT data. The iodine-based oral and intravenous contrast agents we tested seem to be in the range where the effects on attenuation correction factors may be negligible, except for some particular conditions discussed in that Chapter.

Average Organ: Average activity concentration of all pixels in the specified organ

Delineation of organs and ROIs is labor-intensive. The development of automated segmentation algorithms would be helpful for this task.

A similar approach has been used in radiology. A CT scan data set has gray scale values in HU. For diagnosing different lesions in different organs, radiologists will typically look at three sets of images: bone window, soft tissue window, and lung window. The CT value is a representation of a physical property (attenuation coefficients) unique to each tissue type. These windows can be optimized manually by the radiologist; the optimal bone window may be different in health young individuals as opposed to an older individual with osteoporosis. However, each window does not vary greatly among individuals.

In ^{18}F-FDG PET, an analogous window approach is not possible. This is due to ^{18}F-FDG uptake reflecting both normal tissue and tumor physiology. The distribution of activity concentration varies from patient to patient. Given the activity concentrations of

Welc705:peried 96o48126e7clear m

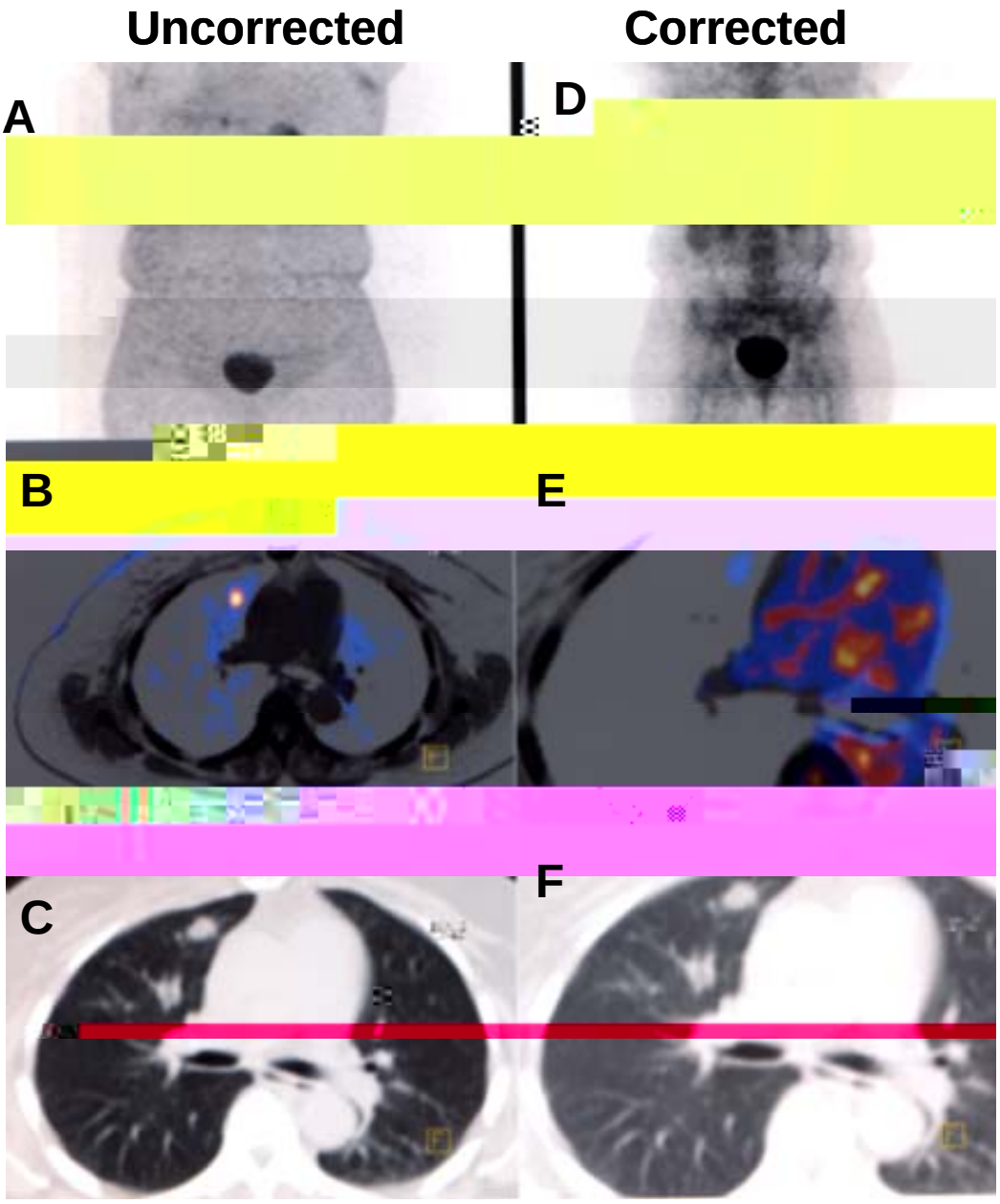

Figure 6-1: An example of the importance in optimizing display windows of both attenuation-corrected and uncorrected image sets to visualize a lesion. A-C: attenuation uncorrected image, D-F: attenuation corrected image. A lesion is visible on A, but not on D. B and E are transaxial fused PET/CT images. The lesion is easily detected on B. Only optimal windowing will allow physicians to visualize the lesion on E. C and F are transaxial CT images. The lesion is not easy to evaluate from CT images only (Courtesy of Steven Bujenovic, M.D.).

References

1. Townsend, D.W., et al., *PET/CT today and tomorrow.* J Nucl Med, 2004. **45 Suppl 1**: p. 4S-14S.

2. Townsend, D.W., T. Beyer, and T.M. Blodgett, *PET/CT scanners: a hardware approach to image fusion.* Semin Nucl Med, 2003. **33**(3): p. 193-204.

3. Lardinois, D., et al., *Staging of non-small-cell lung cancer with integrated positron-emission tomography and computed tomography.* N Engl J Med, 2003. **348**(25): p. 2500-7.

4. Kamel, E.M., et al., *Whole-body (18)F-FDG PET improves the management of patients with small cell lung cancer.* J Nucl Med, 2003.

12. Maisey, M., R.L. Wahl, and S.F. Barrington, *Atlas of clinical positron emission tomography*. 1999, London, New York: Arnold ; Co-published in the USA by Oxford University Press. xi, 346 p.

13. Beyer, T., et al., *Acquisition protocol considerations for combined PET/CT imaging.* J Nucl Med, 2004. **45 Suppl 1**: p. 25S-35S.

14. Cohade, C. and R.L. Wahl, *Applications of positron emission tomography/computed tomography image fusion in clinical positron emission tomography-clinical use, interpretation methods, diagnostic improvements.* Semin Nucl Med, 2003. **33**(3): p. 228-37.

15. Antoch, G., et al., *To enhance or not to enhance? 18F-FDG and CT contrast agents in dual-modality 18F-FDG PET/CT.* J Nucl Med, 2004. **45 Suppl 1**: p. 56S-65S.

16. Nakamoto, Y., et al., *Effects of nonionic intravenous contrast agents at PET/CT imaging: phantom and canine studies.* Radiology, 2003. **227**(3): p. 817-24.

17. Nehmeh, S.A., et al., *Correction for oral contrast artifacts in CT attenuation-corrected PET images obtained by combined PET/CT.* J Nucl Med, 2003. **44**(12): p. 1940-4.

18. Quarantelli, M., et al., *Integrated software for the analysis of brain PET/SPECT studies with partial-volume-effect correction.* J Nucl Med, 2004. **45**(2): p. 192-201.

19. Vogel, W.V., et al., *PET/CT: panacea, redundancy, or something in between?* J Nucl Med, 2004. **45 Suppl 1**: p. 15S-24S.

20. Goerres, G.W., et al., *Accuracy of image coregistration of pulmonary lesions in patients with non-small cell lung cancer using an integrated PET/CT system.* J Nucl Med, 2002. **43**(11): p. 1469-75.

21. Nehmeh, S.A., et al., *Effect of respiratory gating on quantifying PET images of lung cancer.* J Nucl Med, 2002. **43**(7): p. 876-81.

22. Nehmeh, S.A., et al., *Reduction of respiratory motion artifacts in PET imaging of lung cancer by respiratory correlated dynamic PET: methodology and comparison with respiratory gated PET.* J Nucl Med, 2003. **44**(10): p. 1644-8.

23. Valk, P.E., *Positron emission tomography : basic science and clinical practice*. 2003, London ; New York: Springer. xix, 884 p.

24. Tarantola, G., F. Zito, and P. Gerundini, *PET instrumentation and reconstruction algorithms in whole-body applications.* J Nucl Med, 2003. **44**(5): p. 756-69.

39. Nakamoto, Y., et al., *PET/CT: comparison of quantitative tracer uptake between germanium and CT transmission attenuc9015 2 JNucl Med, 2002. 12.007163 78.524 30(attenuc9015 2*

Vita

Yuri Ishihara was born in Kyoto, a unique historical old capital of Japan, where modern technology and Japanese tradition fuse into one. She completed her medical education at Mie University School of Medicine in1993. After graduation she entered her general surgery residency program at the Kyoto Prefectural University of Medicine and Kyoto Second Red Cross Hospital. She became a board certified surgeon of the Japanese Surgical Society in 1998. After she moved to the United States to reside in Baton Rouge, Louisiana, with her husband, she participated in biomedical research at the Pennington Biomedical Research Center as a postdoctoral research fellow under George Bray, MD and David York, PhD from 1999 to 2002 while she was enrolled in undergraduate physics courses at the Louisiana State University. In 2002, upon her award of the Board of Regents fellowship, she started her graduate study in medical physics at Louisiana State University. Her interest in medical physics is applications of medical imaging to improve safety and accuracy of surgical procedures. After graduation, she is joining to Image Guided Therapy Program at Brigham and Women's Hospital, Harvard Medical School, in Boston, Massachusetts as a fellow.